

Article

# Preparation and Characterization of Hybrid Nanocomposites for Dental Applications

Katarzyna Gawdzinska <sup>1</sup>, Sandra Paszkiewicz <sup>2,\*</sup>, Elzbieta Piesowicz <sup>2</sup>, Katarzyna Bryll <sup>1</sup>, Izabela Irska <sup>2</sup>, Agnieszka Lapis <sup>3</sup>, Ewa Sobolewska <sup>3</sup>, Agnieszka Kochmanska <sup>2</sup> and Wojciech Slaczka <sup>1</sup>

<sup>1</sup> Department of Marine Engineering Materials, Faculty of Marine Engineering, Maritime University of Szczecin, Willowa 2–4, 71-650 Szczecin, Poland; k.gawdzinska@am.szczecin.pl (K.G.); k.bryll@am.szczecin.pl (K.B.); w.slaczka@am.szczecin.pl (W.S.)

<sup>2</sup> Department of Polymer Materials, Faculty of Mechanical Engineering and Mechatronics, West Pomeranian University of Technology, al. Piastow 19, 70-310 Szczecin, Poland; senel@zut.edu.pl (E.P.); iirska@zut.edu.pl (I.I.); akochmanska@zut.edu.pl (A.K.)

<sup>3</sup> Department of Dental Prosthetics, Pomeranian Medical University, 70-111 Szczecin, Poland; ag-dent@wp.pl (A.L.); ewasobol@pum.edu.pl (E.S.)

\* Correspondence: spaszkievicz@zut.edu.pl or sandra.paszkievicz@zut.edu.pl; Tel.: +48-91-449-45-89

Received: 28 February 2019; Accepted: 26 March 2019; Published: 1 April 2019



**Featured Application:** The paper presents a recent study on the characterization of the composite materials with improved functional properties that can be used for dental prostheses.

**Abstract:** The study involved research related to the selection of the material with improved functional properties that can be used for dental prostheses. An innovative system of nanofillers, that differ in shape, by means of gelatin-modified halloysite nanotubes (HNTs-g) along with silane-coupled aluminum trihydrate (ATH-sil) was prepared, in order to observe a synergistic improvement of acrylic material (methyl methacrylate with methyl methacrylate monomer (MM/mMM)). Selected mechanical properties of manufactured nanocomposites, along with utilitarian properties, like hardness, buffer solution absorption, and abrasion resistance, along with a fall test from the height of finished products have been discussed. Moreover, the study of the biofilm formation on the surface of dental prostheses confirmed the occurrence of a synergistic improvement of properties and the legitimacy of using modified mineral nanofillers in the form of a hybrid system.

**Keywords:** polymer nanocomposites; synergistic effect; mineral nanofillers

## 1. Introduction

Acrylic materials (in particular methyl methacrylate or poly(methyl methacrylate) (PMMA)) are widely used in many industries, such as automotive and construction, and fields, such as medicine or cosmetology [1]. One can apply them in a wide range of elements for everyday use, such as lampshades, window and car window panes, aerial panels, dental prostheses, sanitary devices, tableware, and other items [2,3]. They are easily formable materials; after heating up to about 150 °C, polished, and machined. Resistant to light, water, diluted acids and alkalis, 40% alcohol, turpentine, gasoline, and mineral oils, acrylic materials dissolve in most organic solvents [3].

Acrylic materials, including PMMA, can be used both independently and in a system with different fillers to form composites or nanocomposites if at least one of the dimensions of the filler reinforcing phase does not exceed 100 nm [4–7]. The composition of the composite should contain up to 30% of the filler in the entire volume of the finished product. The most commonly used fillers in the

preparation of acrylic matrix composites are amorphous silicas [8], fullerenes [9], bentonites [10,11], silver nanoparticles [12], or carbon nanotubes [13,14]. Composite materials are characterized in that they have improved mechanical, thermal, optical, and physicochemical properties compared to the polymer matrix [4–8,13–17]. These materials are usually produced via polymerization process [1,17,18]. As a result of the literature and patent [19–27] it was found that it is possible to obtain polymer nanocomposites with the addition of mineral fillers, such as halloysite nanotubes (HNTs) or alumina trihydrate (ATH). Two patents [28,29] may be found as examples, where the method for preparing a modified halloysite nanotube (mHNTs)/biodegradable polyester composite material has been shown. The method for preparing the composite material comprising the following steps has been presented: Polycondensation of lactic acid (LA) or polylactic surface graft of HNT and subsequently, melt blending, solution blending, or electrospinning the surface graft LA or poly(lactic acid) (PLA) and HNT. Moreover, in [30], the use of polymer matrix composites with HNTs in medicine and dentistry was described. The invention relates to the extended use of poly(methyl methacrylates) (PMMA) with the addition of HNTs as a bone cement for the attachment of the hip, knee, or other implants, the restoration of dental prostheses or the prosthesis itself, and the methods of producing these nanocomposites. This patent also presents the possibilities of introducing antibiotics to PMMA/HNTs composites in the form of bone cement. The beneficial effects of biocompatible HNTs material on bone cement have been proven. Bone cement with the addition of HNTs exhibited higher strength, became resistant to mechanical damage, was characterized by greater adhesion, as well as the possibility of prolonged release of the substance of interest (e.g., antibiotic) [30].

Additionally, one can find the beneficial effect of ATH of various shapes and sizes as a flame retardant agent in the composite systems, based on a matrix of thermoplastic and thermosetting resins [31,32]. The use of ATH in a layered system to improve the properties of a polymer composite intended for coating or supplementing the components of mascara, plaster, paper pulp, cleaning agents, rubber or drilling fluid, and in a cement preparation has been presented [33]. The invention primarily relates to the production of a composite based on poly(vinyl chloride) containing ATH. ATH is also used as an adjuvant in certain vaccines to increase their effectiveness [31]. In turn, Samujlo and Rudawska [21] determined the influence of the incorporation via extrusion of ATH and other auxiliary media into low-density polyethylene (LDPE) on the surface free energy and the roughness of the composite surface. The results confirmed that the introduction of ATH did not have any significant influence on the adhesive properties of the extruded LDPE.

Sometimes, as a result of incompatibility of the composite components, modifications of fillers or the acrylic matrix alone are used in order to combine these components well and to facilitate the combination of these components by changing the contact angle [1,5,25,34,35]. Numerous publications confirmed the effectiveness of the surface modification process of nanotubes, which includes the introduction of a coupling agent in the form of a silane, thanks to which an increase in composite strength is obtained [35–40].

However, despite the interest of numerous research groups with nanocomposites containing mineral fillers, no description of the combination of two types of mineral fillers (HNTs and ATH), that differ in shape, in the polymer matrix (so-called hybrid composites) has been encountered in the literature [26]. In particular, the analysis of the state of the art did not show the use of acrylic matrix nanocomposites with halloysite fillers and ATH for applications in dentistry and prosthetics. The information disclosed relates only to the use of amorphous silicas and bentonites as fillers for the production of a biocompatible bone implant [8,10,11].

HNTs are naturally occurring polymorph of kaolinite, with chemical formula of  $\text{Al}_2\text{Si}_2\text{O}_5(\text{OH})_4 \cdot 2\text{H}_2\text{O}$ , with a dominant hollow tubular morphology [41,42], which, due to their properties and origin, show potential biocompatibility for applications in medicine [22,26]. The same applies to ATH, which can be used as an additive to toothpastes [43]. The halloysite itself is also used in the form of an additive for animal feed [22]. The color of HNT allows one to obtain the proper color of the prosthesis, reduces the translucency of the prosthesis plate, which is especially important for ovoid alveolar appendages, and

the addition of ATH, which is a white powder, does not affect its change. This is an advantage due to the patients’ needs reported in many clinical cases.

Acrylic materials used so far are materials that meet the requirements for materials used in dental prosthetics [2,3,44]. A common problem for the denture user is; however, the brittleness of the material—the destruction of the prosthesis in a catastrophic manner (fall, fracture under pressure). The attempts made so far, and currently used reinforcements, increase the cost of the final product (halloysite is a relatively cheap mineral (ca. 75 Euro/100 g) in relation to, for example, carbon nanotubes (ca. 4000 Euro/100 g), both prices taken from Sigma-Aldrich, and its largest mine is located in Poland in Dunin) or adversely affect the human body (they are allergens). It is; therefore, justified to use methyl methacrylate with methyl methacrylate monomer with the participation of halloysite and aluminum hydroxide, present in the form of a mixture of nanoplatelets and nanotubes, which ensures higher strength of the acrylic material (ultimate strength and elongation to break) for use on dental prostheses. Therefore, the aim of the study was to improve the usable properties, including the mechanical and impact resistance of dental prostheses intended for geriatric patients and the resulting extended life of the product.

## 2. Materials and Methods

### 2.1. Preparation of Polymer Nanocomposites Containing Mineral Nanofillers

In the first stage of the paper, nanocomposites were made via bulk polymerization (canning method commonly used in dental prosthetics) [45,46]. The room temperature during the process was 21 °C. The bulk polymerization was carried out at 60 °C for 3600 s and then at 100 °C for 3600 s. One polymerized methyl methacrylate with methyl methacrylate monomer (MM/mMM) with HNTs, a mineral filler of the formula of  $Al_4Si_4O_{10}(OH)_8 \cdot 4H_2O$ , obtained, in its structure, a number of natural nanotubes with high value of aspect ratio, and platelet packages. HNTs were provided from Intermark, Gliwice (Poland), and, according to the supplier’s data, they exhibit the following characteristics: Bulk density of 450–600 g/dm<sup>3</sup>, color: grey-rusty red, pH: 6–7.5. The concentration of HNTs in the following systems ranged from 1 to 10 mass%. For the whole series of materials (in the percentage range 1%, 2.5%, 5%, 7.5%, 10% mass fraction of HNT in (MM/mMM)), the mechanical properties were tested according to the procedure described below in Section 2.2, to select the most optimal composition for further modifications. The results of these tests are presented in Table 1.

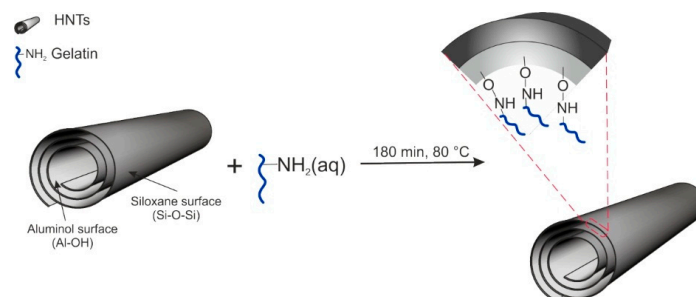
**Table 1.** Selected properties of base material and acrylic-based composites with variable HNTs content.

Sample	$E_t$ (GPa)	$\sigma_B$ (MPa)	$\epsilon_B$ (%)	$E_f$ (GPa)	$\sigma_{fM}$ (MPa)	$\epsilon_{fM}$ (%)	H (Sh <sup>o</sup> D)	KC (kJ/m <sup>2</sup> )	$\rho$ (g/cm <sup>3</sup> )	$\Delta V_{rel}$ (mm <sup>3</sup> )
Base	3.58 ± 0.34	39.29 ± 0.88	1.72 ± 0.15	2.23 ± 0.17	54.67 ± 5.93	2.81 ± 0.28	84 ± 1	12.4 ± 1.2	1.137 ± 0.004	214.98 ± 3.83
1% HNTs	3.98 ± 0.32	24.93 ± 2.13	1.05 ± 0.09	2.48 ± 0.11	42.11 ± 4.54	1.76 ± 0.27	78 ± 4	4.9 ± 0.4	1.124 ± 0.001	233.11 ± 11.72
2.5% HNTs	2.89 ± 0.11	21.93 ± 2.17	0.69 ± 0.07	2.23 ± 0.12	27.88 ± 1.92	1.25 ± 0.38	73 ± 6	3.1 ± 0.2	1.175 ± 0.004	211.26 ± 7.09
5% HNTs	<b>2.63 ± 0.20</b>	<b>27.89 ± 1.55</b>	<b>1.54 ± 0.11</b>	<b>2.32 ± 0.17</b>	<b>44.71 ± 6.44</b>	<b>2.02 ± 0.27</b>	<b>85 ± 1</b>	<b>4.7 ± 0.4</b>	<b>1.137 ± 0.017</b>	<b>207.92 ± 9.57</b>
7.5% HNTs	3.69 ± 0.31	26.51 ± 2.27	0.87 ± 0.08	2.58 ± 0.11	45.77 ± 3.11	1.78 ± 0.17	78 ± 3	4.8 ± 0.7	1.125 ± 0.004	212.45 ± 11.86
10% HNTs	3.17 ± 0.33	29.20 ± 1.99	1.37 ± 0.19	2.63 ± 0.04	38.54 ± 0.56	1.58 ± 0.31	84 ± 1	3.9 ± 0.1	1.141 ± 0.001	211.02 ± 13.59

$E_t$ —tensile modulus;  $\sigma_B$ —stress at break;  $\epsilon_B$ —elongation at break;  $E_f$ —flexural modulus;  $\sigma_{fM}$ —flexural strength;  $\epsilon_{fM}$ —bending deformation; H—hardness; KC—impact strength;  $\rho$ —hydrostatic density;  $\Delta V_{rel}$ —relative volume loss.

Taking into account the relatively high value of elongation at break, hardness, and impact strength, one assumed that the next steps of this experiment, which includes surface modifications of nanofillers, would concern the concentration of 5 mass% of the nanofiller in the polymer matrix. Therefore, in the second stage of work, the halloysite nanofiller was modified in order to improve mechanical properties and to improve the compatibility of the components [47–49]. HNTs have been modified following the procedure described in [50], by introducing into the nanofiller a natural substance, which is a mixture of proteins and peptides (i.e., a gelatin). Bovine gelatin was purchased from Sigma-Aldrich (Saint Louis, MO, USA). Gelatin is a soluble protein obtained by partial hydrolysis of collagen, the main insoluble fibrous protein constituent of bones, cartilage, and skin, with high potential applications in food and pharmaceutical industries [51]. It consists of glycine, proline, and hydroxyproline. In order

to carry out the modification, the mixture of gelatin and halloysite was subjected to the ultrasonic field at the frequency of 250 kHz in demineralized water, in the mass ratio of gelatin to halloysite of 1:2. The reaction was carried out at 80 °C for 3 h. After the reaction was complete, the water was removed (by evaporation) and the dry product was made into a fine powder—milled on a ball mill (Scheme 1).



**Scheme 1.** Schematic illustration of the modification process of HNTs by natural polymer (gelatin).

The halloysite modified with natural polymer (HNT-g) (5 mass%) was introduced into (MM/mMM) by creating a homogeneous dispersion in a high shear mixer and then subjected to bulk polymerization (at 60 °C for 3600 s, then at 100 °C for 3600 s). Nevertheless, the modification of HNTs by gelatin was carried out to improve the quality of dispersion and compatibility between components of the composite, but unfortunately it adversely affected water absorption. That is why, in the third stage of work, nanocomposites based on MM/mMM and 5% of ATH modified with silane (ATH-sil) (Evonik, Germany) was prepared in the form of a powder. This composite was made for comparative purposes to a hybrid composite.

The aim of this work, apart from the presented solutions, is the preparation via bulk polymerization (at 60 °C for 3600 s, and then 100 °C for 3600 min) of polymer hybrid composites based on MM/mMM containing two types of fillers:

- 2.5% HNT + 2.5% ATH-sil and
- 2.5% HNT-g + 2.5% ATH-sil.

## 2.2. Characterization Methods

The dispersion of nanofillers and the nanofillers themselves were observed by scanning electron microscopy (SEM, Hitachi SU-70, Naka, Japan). The samples for SEM analysis were cryofractured in liquid nitrogen and subsequently coated (2–5 nm) in a vacuum with a thin silver film before the tests.

FTIR spectrums were made (Thermo Nicolet 380 apparatus, Thermo Fisher Scientific, Waltham, MA, USA) in the range of wave numbers from 400 to 4000  $\text{cm}^{-1}$  using KBr pellet procedure.

The thermo-oxidative stability of the nanofillers used in this study was evaluated by thermogravimetry (TGA 92-16.18 Setaram, Caluire, France) using the system measuring simultaneously TG-DSC. Measurements were carried out in an oxidizing atmosphere (i.e., dry, synthetic air ( $\text{N}_2:\text{O}_2 = 80:20$  vol.%)). The study was conducted at a heating rate of 10 °C/min in the temperature range of 20–700 °C.

The tensile properties of the prepared composites were measured according to ISO 527 using Autograph AG-X plus (Shimadzu, Kyoto, Japan) tensile testing machine (class 1.0 according to EN 10002-2, ISO 7500-1, BS 1610, ASTM E4, JIS B7721), equipped with a 1 kN Shimadzu load cell, an optical extensometer (class 0.5 according to ISO 9513), and the TRAPEZIUM X computer software (version 1.4.5, Shimadzu, Kyoto, Japan), operated at a constant crosshead speed of 1 mm/min. Measurements were performed at room temperature on the dumbbell samples with the grip distance of 30 mm. Seven measurements were conducted for each dumbbell-shaped sample (type A3), and the results were averaged to obtain a mean value. Results, taking into account standard uncertainty of measurement (according to Guide to the Expression of Uncertainty in Measurement, ISO, Switzerland 1995), for chosen qualities of researched materials are presented in Tables 1 and 2.

The flexural properties were measured according to ISO 178 using Autograph AG-X plus (Shimadzu) testing machine (class 1.0 according to EN 10002-2, ISO 7500-1, BS 1610, ASTM E4, JIS B7721), equipped with a 1 kN Shimadzu load cell, operated at a constant crosshead speed of 1 mm/min. Measurements were performed on the samples with the dimensions of:  $l = 80 \pm 2$  mm,  $b = 10 \pm 0.2$  mm,  $h = 4 \pm 0.2$  mm.

The impact strength was determined by Charpy method according to the standard ISO 179-1/1eU), type of the sample: 1 ( $l = 80 \pm 2$  mm,  $b = 10 \pm 0.2$  mm,  $h = 4 \pm 0.2$  mm), edge impact (e), no notch (U).

Hardness was determined by Shore method according to a standard EN ISO 868:2003 on a Zwick 3100 Shore D tester (Zwick GmbH, Ulm, Germany).

Determination of abrasion resistance was carried out using a Schopper-Schlobach (VEB Thüringer Industriewerk, Thüringer, Germany) with a rotating drum in accordance with ISO 4649: 2002 (E). Test samples: cylinder with a diameter of  $16 \text{ mm} \pm 0.2$  mm and a height of at least 6 mm. The method B was used, with the sample rotating, the pressing force to the barrel  $10 \text{ N} \pm 0.2$  N. The density necessary to calculate the volume loss of mass was determined by the hydrostatic method (according to ISO 2781). Distilled water was used as an immersion liquid. The results are presented as the relative volume loss ( $\Delta V_{rel}$ ) expressed in  $\text{mm}^3$ , calculated according to the formula:

$$\Delta V_{rel} = \frac{\Delta m_t \times \Delta m_{const}}{\rho_t \times \Delta m_r} \quad (1)$$

where:

$\Delta m_t$ —mass loss of the tested rubber sample, in mg;

$\Delta m_{const}$ —determined value of mass loss of a rubber sample made of a reference composition, in mg;

$\rho_t$ —the density of the tested rubber, in  $\text{mg}/\text{mm}^2$ ;

$\Delta m_r$ —mass loss of a rubber sample made of a reference composition, in mg (212 mg).

The absorption testes were carried out in accordance with the standard ISO 62. Six materials were subjected to the study (4 samples each). The absorption was tested in a buffer solution (PBS, Phosphate Buffered Saline, Sigma Aldrich, Merck KGaA, Darmstadt, Germany) with pH equal to 7.4. The samples were dried under vacuum for 24 h at  $50^\circ\text{C}$  before testing, and then were weighed ( $m_1$ ). The samples were then placed in a buffer solution and left for 120 h in a chamber at  $60^\circ\text{C}$ . After 120 h, the samples were thermostated in distilled water (room temperature) for 15 min, dried, and weighed ( $m_2$ ). The samples were then dried for 24 h at  $50^\circ\text{C}$  and weighed ( $m_3$ ). The absorbency of the samples was calculated from the formula (as  $m_3 > m_1$ ):

$$A = \frac{m_2 - m_3}{m_1} \cdot 100\% \quad (2)$$

where

- $m_1$ —mass of the sample after drying, before the absorbency test;
- $m_2$ —mass of the samples after absorbency test;
- $m_3$ —mass of the sample after absorbency test and after drying.

The following reference strains were used in the microbiological study: *Staphylococcus aureus* ATCC 25923, *Escherichia coli* ATCC 25922, *Pseudomonas aeruginosa* ATCC 27853, *Enterococcus faecalis* ATCC 29212, and *Candida albicans* ATCC 10231. For the breeding of bacteria, Columbia agar medium with the addition of 5% sheep blood was used (bioMérieux, Warsaw, Poland), while for the cultivation of yeast, the Sabouraud substrate (bioMérieux, Warsaw, Poland) was used. Incubation was carried out at  $37^\circ\text{C}$  for 24 h under aerobic conditions. The examination of biofilm formation on the surface of prosthetic materials was conducted by two methods:

- Quality method

The study of the formation of bacterial and fungal biofilms on the surface of prosthetic materials cut to 1:1 cm was estimated using the qualitative method—Richards [52]. A suspension with a density of 1.0 on the McFarland scale was prepared from a 24-h culture grown on a TSB medium, and then sterile specimens of prosthetic materials were placed in. After a 24-h incubation at 37 °C, the samples were washed three times with NaCl and 1 drop of 1% 2,3,5-triphenyltetrazolium chloride (TTC) solution was added to them. The samples were again subjected to 24-h incubation at 37 °C. All tests were carried out in duplicate. The results were read using a three-color scale of color intensity.

- Quantitative method

The study of the formation of bacterial and fungal biofilms on the surface of prosthetic materials cut 1:1 cm by the quantitative method was determined according to Maczynska et al. [53]. A suspension of 1.0 McFarland density was prepared in the same manner as in the qualitative method, then the test materials were placed therein and incubated for 24 h at 37 °C. The next step was to place the prosthetic samples in a 0.5% solution of saponin and shake for 60 s to detach the biofilm cells. The suspension obtained in this way was plated at successive dilutions, 100 µL per Columbia agar medium with 5% sheep blood and Sabouraud medium, and again incubated for 24 h at 37 °C. The results were read after calculating the number of microbial cells detached from the surface of composite materials.

### 3. Results and Discussion

#### 3.1. Characterization of Nanofillers

Figure 1 displays scanning electron microscopy (SEM) images of HNTs (a), modified HNTs with gelatin (b), and silane-modified ATH (c). As one can see in SEM images (a) and (b) the surface of the modified HNTs with gelatin became rough compared with the raw HNTs. Therefore, the results demonstrated that gelatin was successfully grafted on the surface of HNTs. The SEM image (Figure 1a) of HNTs reveal that the majority of HNTs existed in a tubular shape. The presence of short tubular HNTs, semi-rolled HNTs, and sheet-like HNTs were visible. A mean particle size of ca. 1.5 µm and lengths ranging from 500 nm to 3 µm were determined. In turn, the morphology of the as-received silane-modified ATH observed by SEM (Figure 1c) was similar to the ones obtained from the manufacturer and provided in the technical data sheet. Particles were not uniform in shape and they exhibited an almost smooth surface.

The above-mentioned observations were further confirmed by FTIR and TGA analyses (Figure 2). Figure 2a illustrates the TGA curves of pristine HNTs and gelatin-modified HNTs. In the curve of pristine HNTs nanotubes, one major mass loss was resolved in the temperature range of 380–600 °C. This mass loss has been assigned to the dehydroxylation of structural Al-OH groups of halloysite [54,55]. Another mass loss, observed in the range 23–120 °C, corresponded to the loss of adsorbed water (surface and interlayer) [54]. On the other hand, for the gelatin-modified HNTs, three mass losses were resolved. The first mass loss in the range 23–125 °C was due to physically adsorbed water, the second mass loss occurring from approximately 250–400 °C was due to decomposition of the grafted gelatin [56], and the last mass loss over the range 435–675 °C corresponded to dehydroxylation of the residual structural Al-OH groups. Thus, one can make an important conclusion, that HNTs have been successfully modified with gelatin, which will also be evidenced by the FTIR analysis. Figure 2b presents the FTIR spectra of the pristine HNTs and gelatin-modified HNTs. Both pristine HNTs and modified HNTs showed strong peaks at 3697 and 3615 cm<sup>-1</sup>, respectively, which correspond to the stretching vibration of Al-OH groups in the inner surface; at 1028 and 909 cm<sup>-1</sup>, peaks corresponded to Si-O stretching and Al-OH bending vibrations, respectively [57]. Meanwhile, minor peaks at 2932, 2359, 1680, and 1540 cm<sup>-1</sup>, corresponding to C-H stretching vibration, carbonyl group [58], hydrogen bonding of COOH groups [59], N-H bending vibration [60], and C-N stretching vibration [61], respectively, could be seen in the gelatin-modified HNTs spectrum rather than in the spectrum of pristine HNTs.

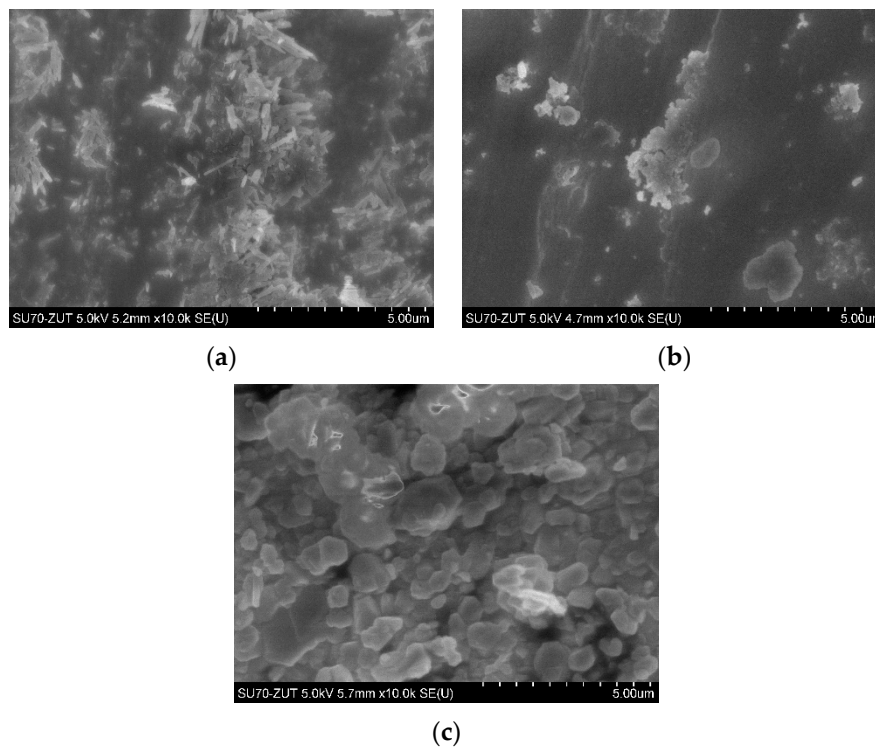


Figure 1. SEM micrographs of: HNTs (a), HNTs-g (b), and ATH-sil (c).

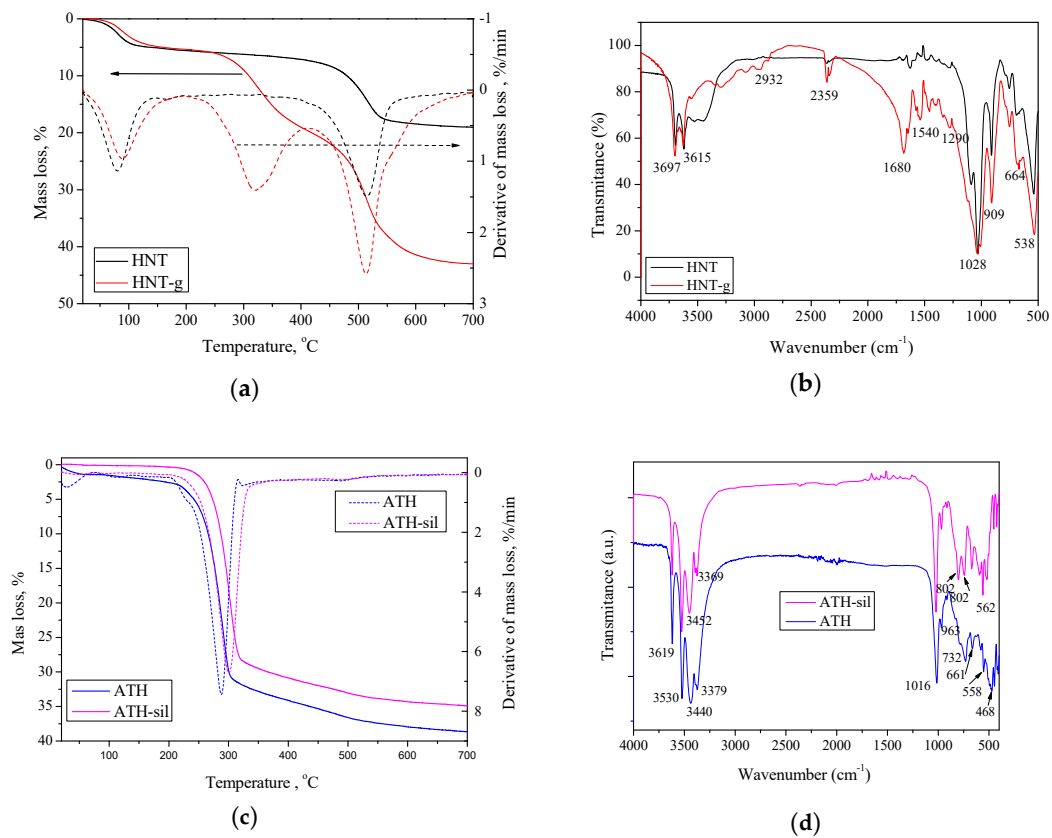


Figure 2. TG curves (a) and FTIR spectra (b) of pristine HNTs and gelatin-modified HNTs; TG curves (c) and FTIR spectra (d) of pristine ATH and silane-modified ATH.

As mentioned above, thermal properties of modified nanofillers are related to the nature of surfactants used. Therefore, on TGA curves for pristine ATH and silane-modified ATH (Figure 2c),

one can observe clear differences. For pristine ATH, two mass losses were visible: The first one, in the temperature range of 20–165 °C, corresponded to the loss of adsorbed water [62], and the second major mass loss, in the temperature range of 180–600 °C, corresponded to the decomposition of surfactant molecules [63]. In turn, the silane-modified ATH decomposed in one major step; however, its decomposition temperature was improved by about 20 °C. It was especially well observed at the derivative curve of TG, where the maximum thermal decomposition was shifted from 288 °C (pristine ATH) to 300 °C for the modified ATH. Moreover, a very high char residue value for both fillers was observed. Such improvement confirms the legitimacy of using silane-modified ATH, as it is well-known that such surface treatment affects the dispersibility of the filler, water absorption of the final material, and improves the mechanical properties [64]. Moreover, Figure 2d shows the FTIR spectra of pristine ATH and silane-modified ATH. In the FTIR spectra of both fillers, the bands at 661  $\text{cm}^{-1}$  and 963  $\text{cm}^{-1}$  were related to the Al–O stretching vibrations [65]; the strong band at 1016  $\text{cm}^{-1}$  was related to the bending vibrations of the C–O bond [66]. Compared to the unmodified ATH, silane-modified ATH exhibited some new peaks, such the stretching  $\text{NH}_2$  vibration at 3452  $\text{cm}^{-1}$ , which was due to surface modification by the silane coupling agent. Moreover, ATH-sil exhibited some extra peaks at 802, 661, and 562  $\text{cm}^{-1}$ , while some peaks (3379  $\text{cm}^{-1}$  and 3440  $\text{cm}^{-1}$ ) shifted to higher frequencies. These observations, along with TGA and SEM analyses, suggest that the silane modification conducted by the manufacturer was successfully prepared and indeed authors used silane-modified ATH to prepare the polymer hybrid nanocomposites.

### 3.2. Dispersion Characteristics

The surface modification of nanoparticles by chemical treatments (such as the functionalization by natural polymers or the absorption of silane coupling agents) is a useful method to improve the dispersion stability of nanoparticles in a polymer matrix. Thus, the functionalization of HNTs is extremely important for processing and enhancing the properties of HNTs/polymer nanocomposites. The polymer nanocomposites based on modified nanotubes exhibited improved mechanical and thermal properties, because the functionalization improved the dispersion and stress–strain characteristics [67]. In addition, Plueddemann [64] confirmed that the modification of particles' surfaces using silane coupling agents cause improvement of the compatibility between the particle and polymer surfaces and; thus, the properties of composite materials. In the present study, composites containing 5% pristine HNTs, 5% of gelatin-modified HNTs (HNTs-g), 5% of silane-modified ATH, and 2.5% of gelatin-modified HNTs + 2.5% of silane-modified ATH were observed by SEM (Figure 3). The effect of the modification of nanofillers was depicted. HNTs exhibited a high specific surface area, which was favorable for interfacial interaction with the polymer matrix, thus promoting stronger bonding at the interfaces. One can find that unmodified HNTs seemed to be completely covered by the polymer matrix (Figure 3a). As expected, the chemical modification of HNTs by natural polymer (gelatin) affected the dispersion of nanofiller in the polymer matrix. At the same magnification (20,000 $\times$ ), one can find that the morphology of the sample was changed completely, and single nanotubes sticking out from the matrix could be seen (indicated with arrows, Figure 3b). In turn, the SEM image of polymer nanocomposite with 5% of silane-modified ATH revealed a peel-like and a loose microstructure with leaflet pattern. Such magnification (20,000 $\times$ ) allows one to observe the close stacking of a layered structure with a smooth surface (marked with a circle, Figure 3c). Moreover, Figure 3d presents the SEM image of the hybrid nanocomposite containing both modified nanofillers: HNTs-g and ATH-sil. At the magnification of 10,000 $\times$ , both structures were clearly visible (i.e., well-dispersed HNTs-g along with the layered structure of ATH-sil). Herein, it can be concluded that ATH-sil appeared to be “more complex” with the matrix, while the nanotubes, distributed evenly in the matrix, appeared to protrude from one end and the other to be anchored in the polymer. Nevertheless, on the basis of the morphological observations and the obtained proper nanoparticles' dispersion, an improvement in the functional properties (mechanical, biological activity) of the finished product, in the form of a denture, could be expected.

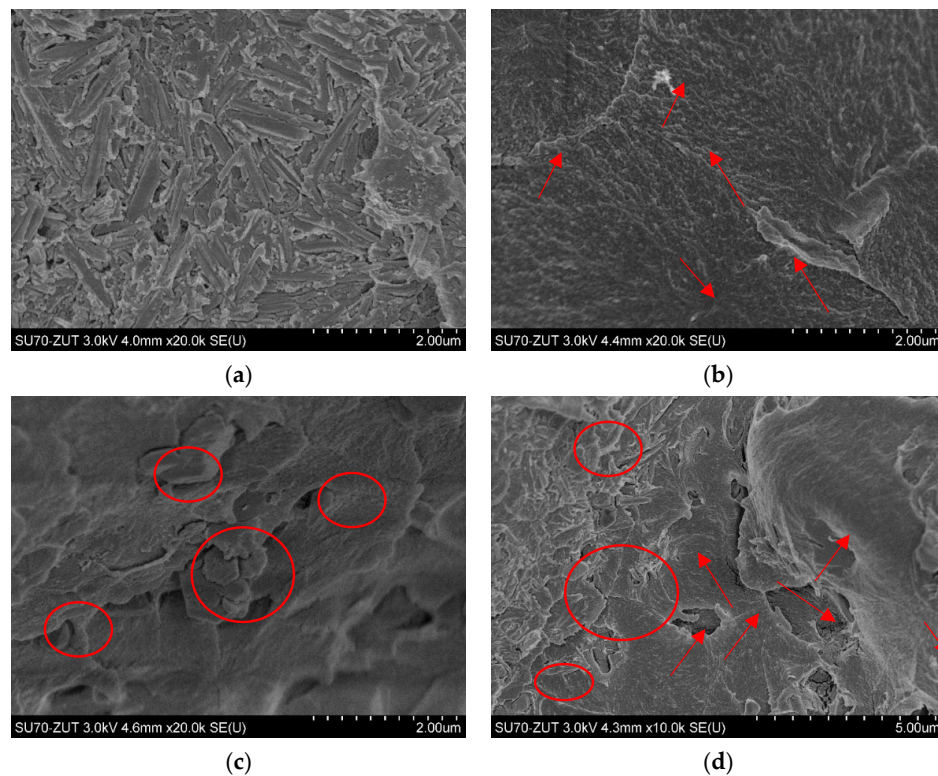


**Figure 3.** SEM micrographs of fracture surfaces of the composites containing: 5% HNT (a); 5% HNT-g (b); 5% ATH-sil (c), and 2.5% HNT-g + 2.5% ATH-sil (d).

### 3.3. Mechanical Properties

As mentioned above, the functionalization of nanofillers and its effect on dispersion in a polymer matrix are supposed to improve mechanical properties. Two methods were employed to investigate the mechanical properties: tensile test and bending test (Figure 4, Table 2). Results show that the modification of both HNTs and ATH slightly reduced the mechanical properties of acrylic material. In addition, in Figure 4c,d, it is visible, that properties deviated from the average value very symmetrically and there were no typical, separated values that would exceed the specified deviation. As a result of the analysis of the obtained results, it could be observed that the incorporation of mineral nanofillers caused the improvement of flexural modulus and flexural strength. Despite the fact that the value of tensile modulus was decreased, at the same time the value of stress at break was increased in the presence of nanoparticles. For the composites containing 5 wt.% of HNTs-g, there was an approximate 50% decrease in tensile strength; however, at the same time a 91% increase in elongation was seen, which justifies the modification of the surface of HNTs. In general, all composites exhibited higher values of  $E_f$  and  $\sigma_{fM}$ , with a slight decrease in the value of deformation when bending, while the greatest improvement was seen for the sample containing 2.5% of HNTs-g + 2.5 wt.% of ATH-sil, thus proving the emergence of a positive hybrid effect. Similar observations were made in the case of the improvement of flexural modulus and flexural strength. Moreover, the incorporation of modified nanofillers caused the increase of hardness, whereas the value of hydrostatic density increased slightly, which was probably due to the basis of mixtures, where the nanoparticles exhibited a higher density than the acrylic material. The modification of nanofillers resulted in the enhancement of particle dispersion stability, thus producing chemical interactions (physical and chemical bonds) with the acrylic matrix. Surface-modified HNTs and ATH can produce stress damping centers in the polymer matrix that dissipate the applied stress and, in this manner, prevent the composite brittleness. The interfacial interactions between the nanofillers and the acrylic materials and the high flexural modulus of nanocomposites confirmed the observation of the improvement of impact strength. In addition, it is also worth mentioning that the incorporation of mineral nanofillers affected two

important utilitarian properties in the dental prosthesis (i.e., abrasion resistance and buffer solution absorption (BSA)). One can observe that the incorporation of modified nanofillers affected the BSA and abrasion resistance, wherein the most promising of all analyzed systems turned out to be a hybrid of two modified nanofillers (i.e., 2.5% HNTs-g + 2.5% AHT-sil).

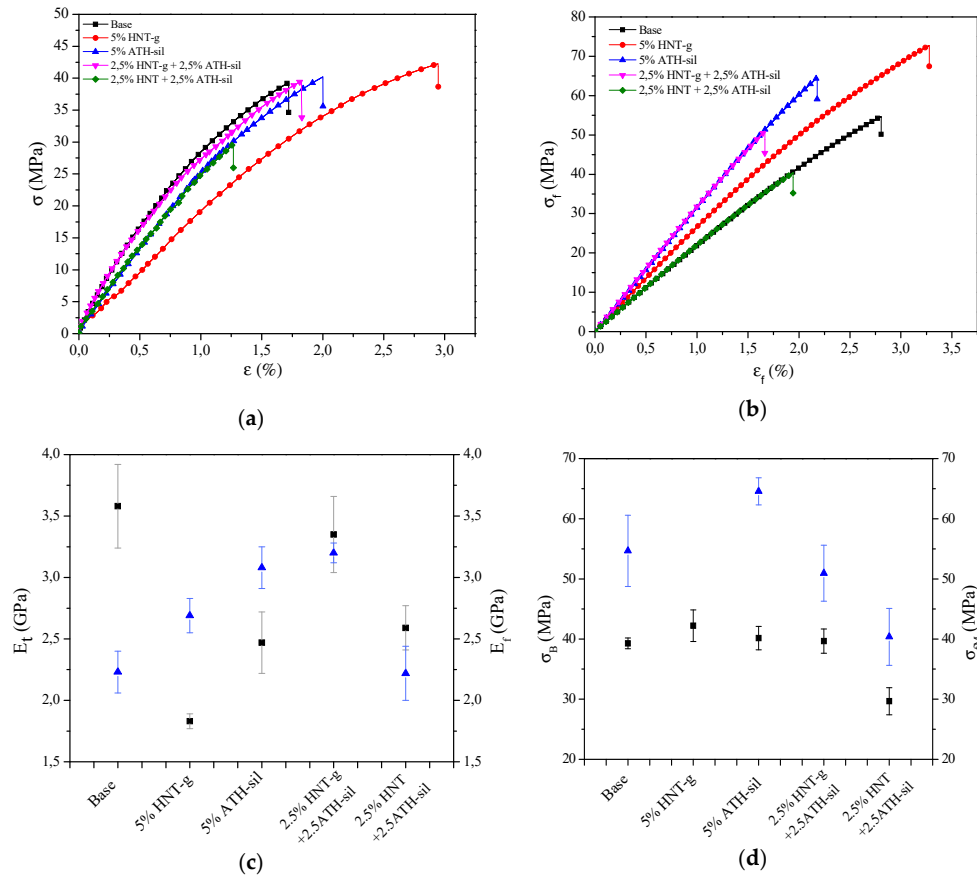


**Figure 4.** Representative stress–strain curves for the series polymer nanocomposites recorded during static tensile test (a) and static bending test (b); comparison of the values of elastic and flexural moduli (c) and stress at break and flexural strength (d) for polymer nanocomposites in relation to the base material.

**Table 2.** The selected physical properties of the base material (MM/mMM) and composites containing modified and unmodified nanofillers.

Sample	$E_t$ (GPa)	$\sigma_B$ (MPa)	$\epsilon_B$ (%)	$E_f$ (GPa)	$\sigma_{fM}$ (MPa)	$\epsilon_{fM}$ (%)	H (Sh°D)	KC (kJ/m <sup>2</sup> )	$\rho$ (g/cm <sup>3</sup> )	$\Delta V_{rel}$ (mm <sup>3</sup> )	BSA (%)
Base	3.58 ± 0.34	39.29 ± 0.88	1.72 ± 0.15	2.23 ± 0.17	54.67 ± 5.93	2.81 ± 0.28	84 ± 1	12.4 ± 1.2	1.137 ± 0.004	214.98 ± 3.83	2.75 ± 0.20
5% HNT	2.63 ± 0.20	27.89 ± 1.55	1.54 ± 0.11	2.32 ± 0.17	44.71 ± 6.44	2.02 ± 0.27	85 ± 1	4.7 ± 0.4	1.137 ± 0.017	207.92 ± 9.57	2.17 ± 0.07
5% HNT-g	1.83 ± 0.06	42.22 ± 2.62	2.95 ± 0.13	2.69 ± 0.14	72.73 ± 6.75	3.28 ± 0.44	82 ± 1	6.6 ± 0.5	1.171 ± 0.001	194.49 ± 7.06	2.25 ± 0.13
5%ATH-sil	2.47 ± 0.25	40.15 ± 1.95	2.00 ± 0.12	3.08 ± 0.17	64.56 ± 2.24	2.18 ± 0.12	88 ± 2	9.3 ± 0.7	1.204 ± 0.001	178.94 ± 63.04	1.76 ± 0.09
2.5%HNT-g + 2.5%ATH-sil	3.35 ± 0.31	39.66 ± 2.03	1.83 ± 0.14	3.20 ± 0.08	50.95 ± 4.65	1.66 ± 0.18	86 ± 2	5.6 ± 0.6	1.196 ± 0.001	187.05 ± 4.85	2.07 ± 0.09
2.5%HNT + 2.5%ATH-sil	2.59 ± 0.18	29.67 ± 2.27	1.27 ± 0.13	2.22 ± 0.22	40.37 ± 4.73	1.94 ± 0.12	88 ± 1	6.3 ± 0.9	1.153 ± 0.001	198.28 ± 7.98	1.92 ± 0.07

$E_t$ —tensile modulus;  $\sigma_B$ —stress at break;  $\epsilon_B$ —elongation at break;  $E_f$ —flexural modulus;  $\sigma_{fM}$ —flexural strength;  $\epsilon_{fM}$ —bending deformation; H—hardness; KC—impact strength;  $\rho$ —hydrostatic density;  $\Delta V_{rel}$ —relative volume loss; BSA—buffer solution absorption.

Moreover, from the obtained composite materials, one has prepared dental prostheses (Figure 5). Finished products were subjected to a fall test from a height. This trial was a simulation of the fall and permanent damage of the dental prosthesis that happens frequently (on average three times a year for one patient—data provided by the Department of Dental Prosthetics, Pomeranian Medical University in Szczecin—analyzed group: 1500 people), especially in geriatric patients. The fall test from the height

was carried out on a self-constructed stand (Figure 6) utilizing inertial force. Three dentures made of the materials presented in Table 3 were selected for the fall test from height. This table also contains numerical values of cracks for each group of materials, which were recorded by analyzing the denture surface with a stereological microscope at a fall from 50, 100, and 150 cm. The height values were adjusted to the actual conditions of use of the dental prosthesis by the patient and, in the opinion of the authors, were sufficient.

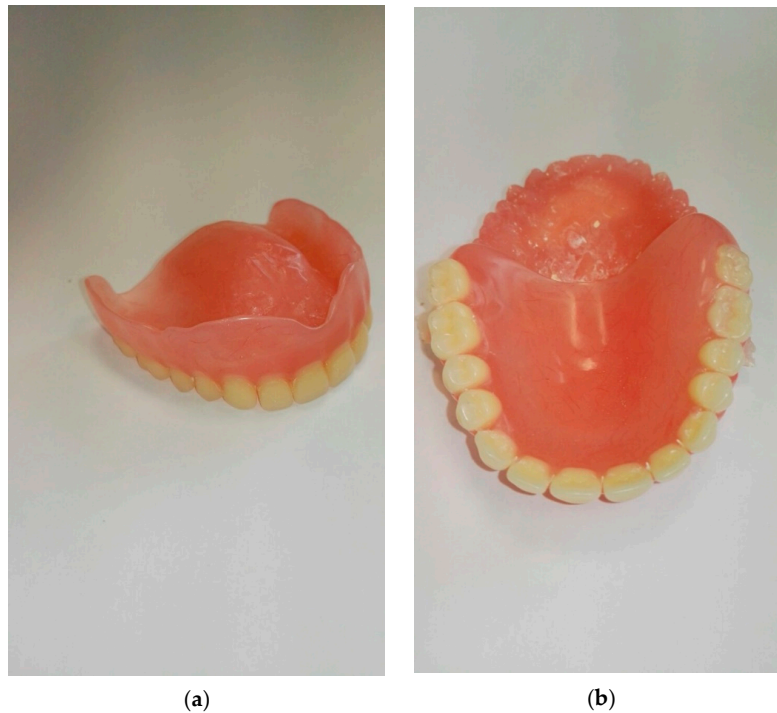


**Figure 5.** The image of the prepared dental prosthesis made from hybrid composite: base + 2.5% HNT-g + 2.5% ATH-sil, view of the upper (a) and lower part (b) of the complete denture prosthesis.

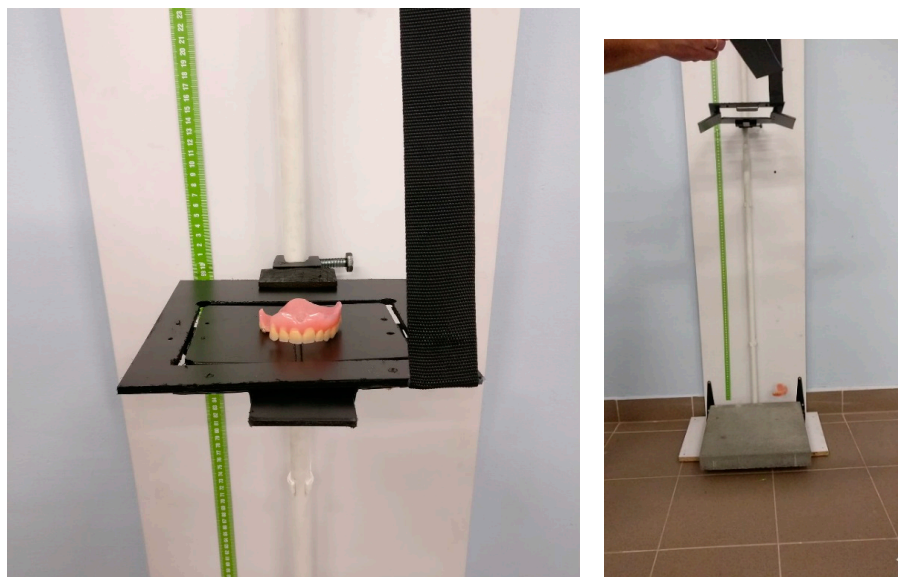


**Figure 6.** The view of the created test bench for the fall from height. The substrate (the material on which the dental prosthesis falls) was a paved concrete slab (B20 concrete class according to PN-B-03264: 2002/ Ap1 2004). Each product was placed on two perpendicular platforms and the hinges were released, which caused the product to fall from a certain height in accordance with the principle of gravity.

**Table 3.** Fall test, from a height of 50, 100, and 150 cm, of dentures with a specific composition (numerical values in each field are the average of three trials).

Height [cm] Sample	50	100	150
Base	2	2	3
Base + 5% HNT	0	0	1
Base + 5% HNT-g	0	0	0
Base + 5% ATH-sil	0	0	1
Base + 2.5% HNT-g + 2.5% ATH-sil	0	0	0
Base + 2.5% HNT + 2.5% ATH-sil	0	0	0

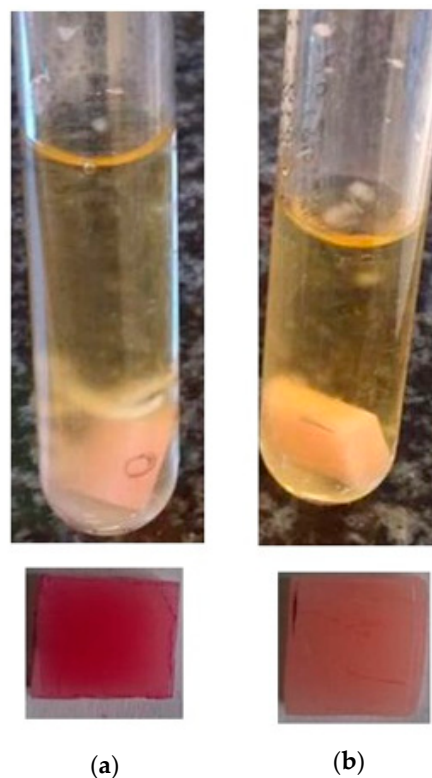
### 3.4. Study of Biofilm Formation on the Surface of Prosthetic Materials

Figure 1 displays scanning electron microscopy (SEM) images of HNTs (a), modified HNTs with gelatin (b), and silane-modified.

Biofilm formation on the surface of prosthetic materials (1:1 cm): reference sample and composites with the addition of mineral nanoparticles were initially assessed using the qualitative method (Richards) and then with the quantitative method. In the Richards method, the following classification of results was adopted depending on the color of the prosthetic material:

- (–)—strain not forming the biofilm (corresponded to the lack of cells)
- (+)—strain weakly forming the biofilm (corresponded to  $10^3$ – $10^4$  CFU/mL)
- (++)—strain strongly forming the biofilm (corresponded to  $10^5$ – $10^6$  CFU/mL)
- (+++)—strain strongly forming the biofilm (corresponded to  $10^7$ – $10^8$  CFU/mL)

On the basis of the conducted research, differences in biofilm estimation were observed in the qualitative and quantitative method, but in both methods there was no complete lack of biofilm (Table 4, Figures 7 and 8).



**Figure 7.** Analysis of the impact of composite materials: base material (a) and hybrid composite base + 2.5% HNT-g + 2.5% ATH-sil (b), against the *C. albicans* strain—qualitative method.

**Table 4.** Classification of biofilm formation for individual strains.

		Strain Used in Biofilm Analysis				
		<i>C. albicans</i>	<i>S. aureus</i>	<i>P. aeruginosa</i>	<i>E. faecalis</i>	<i>E. coli</i>
<b>Samples</b>	Base	+++	++	++	+	+
	Base + 5% HNT	++	++	++	+	+
	Base + 5% HNT-g	+++	++	++	+	+
	Base + 5% ATH-sil	++	++	+	+	+
	Base + 2.5% HNT-g + 2.5% ATH-sil	++	++	+	+	+
	Base + 2.5% HNT + 2.5% ATH-sil	+	++	+	+	+

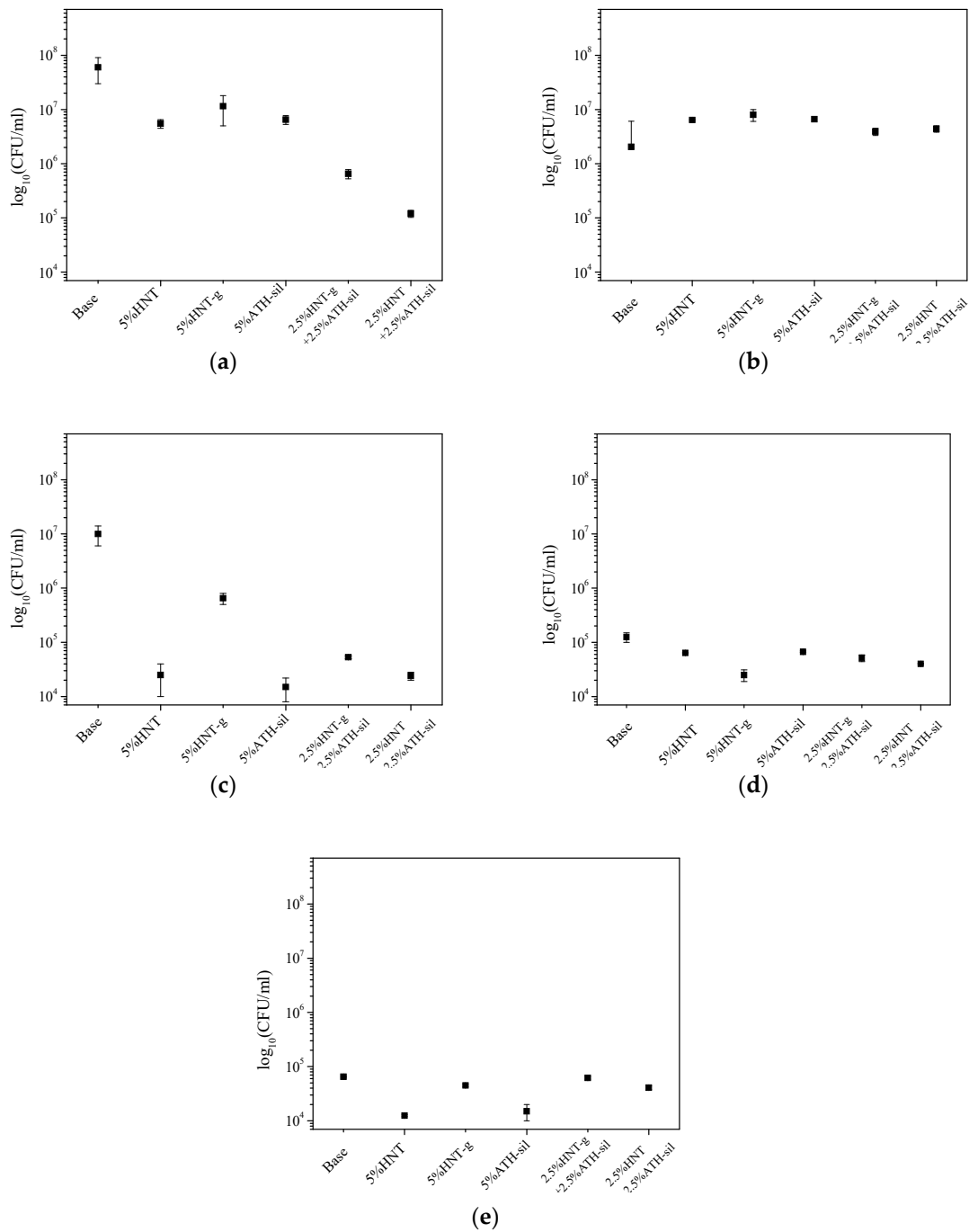


**Figure 8.** Analysis of the impact of the base material and the prepared composites against the following strains: *C. albicans* (a), *S. aureus* (b), *P. aeruginosa* (c), *E. faecalis* (d), and *E. coli* (e)—quantitative method.

### 3.4.1. Quality Method

Three strains were classified as strongly forming the biofilms: *C. albicans* (+++) (Figure 7a), *S. aureus* (++) and *P. aeruginosa* (++)). In the case of yeast, the addition of a hybrid system of modified nanofillers, (i.e., 2.5% HNTs-g + 2.5% ATH-sil) reduced the biofilm formation to scale (+) (Figure 7b), corresponding to strains weakly forming biofilms. A similar situation concerned *P. aeruginosa*, which, in the presence of the composite material with the addition of HNTs (modified and unmodified), strongly produced biofilms (++)), while the addition of silane-modified ATH caused its weaker production (+). In *S. aureus* (++)), *E. faecalis* (+), and *E. coli* (+) strains, no differences in biofilm formation were observed if compared to neat acrylic material (base) and composites containing mineral nanofillers.

### 3.4.2. Quantitative Method

Analyzing the results of biofilm formation using the quantitative method, it was noted that the addition of mineral nanofillers to acrylic material caused a reduction in biofilm formation on the surface of materials in the presence of all microorganisms, although only in the case of *C. albicans* and *P. aeruginosa*, these results corresponded with the qualitative method. In the case of other strains, only minimal differences in biofilm formation were observed, if comparing the base material to the ones containing mineral nanofillers. Researchers are trying to find out the way of improving the dental materials properties, so that the biofilm concentration will be reduced. It is important due to the growing number of patients with stomatitis. Valdez-Salas et al. [68] investigated the influence of TiO<sub>2</sub> nanopatterning on *C. albicans* adhesion. The results received by scanning electron microscopy demonstrated that the applied method could improve the early fungal resistance according to *C. albicans* colonization of dental implants. Changing biofilm accumulation by coating material with silver was investigated both for titanium and acrylic resin. For titanium (electrodeposition of silver nanoparticles), silver deposition did not reduce biofilm adhesion compared to non-coated surfaces [69]. On the other hand, Li Z. et al. [70], in their work about denture base acrylic resin containing silver nanoparticles, concluded that the activity and the amount of *C. albicans* biofilm decreased with the increase of nano-silver solution concentration. Anti-adhesion properties occurred with the 5 wt.% and higher concentration of nano-silver in acrylic resin, and the dependence was proportional. Shu Z. et al. [71] investigated the antibacterial activity of Ag-ZnO/HNTs (halloysite nanotubes supported Ag and ZnO nanoparticles). Observational results of *E. Coli* morphology and surface structure confirmed their hypothesis. They concluded that the complex-containing halloysite has the capacity to inhibit bacteria growth. These results confirm the earlier findings of Yu L. et al. [72], who also proved the antibacterial properties of halloysite while investigating an Ag/HNTs/rGo complex. Cervini-Silva et al. [73], on the other hand, presented anti-inflammatory properties of halloysite surfaces. Halloysite showed greater anti-inflammatory activity in comparison with other clay minerals. Comparing with our study, we also found the dependence for bacteria/fungi inhibition—*C. albicans* and *P. aeruginosa* accumulation. Adding halloysite to the acrylic resin caused proportional reduction of biofilm at the surface of studied materials. The results were presented using a popular chart, a so-called “Tukey boxplot” (Figure 8), in which the values of bars were determined by one and a half value of the quartile range (but only on condition that the minimum and maximum were greater than these values; otherwise the description ends with minimum and maximum values).

## 4. Conclusions

Literature analysis on similar materials (with a matrix of polyesters or polymethacrylates) and on our own laboratory experiments confirmed that:

- It is possible to modify the methyl methacrylate with the methyl methacrylate monomer (MM/mMM) by the addition of HNTs, in the proportion of 1–10 wt.%;
- It is possible to prepare the polymer hybrid nanocomposite based on MM/mMM containing 2.5% HNT + 2.5% ATH-sil;

- It is possible to modify the same hybrid nanocomposites, except that the halloysite nanofiller was modified with natural polymer (gelatin);
- The incorporation of two mineral nanofillers into the polymer allows one to obtain nanocomposites with enhanced functional properties compared to the polymer matrix.

The best functional properties were obtained for a hybrid nanocomposite containing 2.5% of gelatin-modified HNT and 2.5% of silane-modified ATH. The obtained results indicate improvement of mechanical characteristics for nanocomposites with the addition of modified nanofillers, including the improvement of stress break and the increase of flexural strength and impact resistance, while maintaining a relatively low-density ca.  $1.196 \pm 0.001$ . The lowest weight loss in the abrasion test exhibited a composite containing 5% ATH-sil, resulting in an increase in abrasion resistance of about 17% compared to the base material. Slightly worse (by 3.5%) abrasion resistance, than the composite containing 5% of ATH-sil, was shown by the hybrid composite with the addition of modified nanofillers (2.5% HNT-g + 2.5% ATH-sil). These properties, in the case of composites, depend on the degree of the dispersion of nanofiller in the matrix. Due to the low content of hydroxyl groups on the surface of the mineral, HNT disperse very well in polymer matrices, especially after modification with a natural polymer (gelatin). The assessment of the fall from the height of finished denture products has confirmed the goal of producing hybrid nanocomposites based on an acrylic matrix. The largest number of cracks was recorded for dental prostheses made of the base material (MM/mMM). This is confirmed by the experience of the authors in the field of dental prosthetics. Often for geriatric patients one can observe the fall of dentures and their impact on the sink (simulation: 50 cm—two cracks) or on the bathroom glaze (simulation: 100 cm—two cracks; 150 cm—three cracks). In the case of composites containing HNTs and/or ATH, there were no cracks in the fall test, except for the prosthesis made of a nanocomposite containing silane-modified ATH, falling from a height of 150 cm. An additional advantage of the produced materials is the impact on the reduction of biofilm formation, especially in the case of yeast, and the limitation of biofilm formation for selected bacterial strains.

## 5. Patents

The patent application P.428914 titled “Modified methyl methacrylate with methyl methacrylate monomer” resulted from the work reported in this manuscript.

**Author Contributions:** K.G. wrote the general draft of the paper, was responsible for preparation of the patent application, and helped in the discussion on the results; S.P. is the main author of the paper, she wrote the final draft of the manuscript, was responsible for planning the experiment on the modification of nanofillers, and for the discussion of the results; E.P. was responsible for carrying out the modification of nanofillers and the preparation of polymer nanocomposites; K.B. carried out the fall test from the height; I.I. performed the tensile analysis on the samples, along with measurements of hardness, absorbency, impact, density, and wear resistance; A.L. prepared the dental prostheses for the final test and carried out biological tests; E.S. supervised the discussion on the biological tests; A.K. prepared the samples for SEM analysis and performed the analysis on the samples; W.S. helped in the discussion of the results.

**Funding:** This research received no external funding.

**Conflicts of Interest:** The authors declare no conflicts of interest.

## References

1. Ashcroft, W.A. *Industrial Polymer Applications: Essential Chemistry and Technology*, 1st ed.; Royal Society of Chemistry: London, UK, 2017.
2. Pawar, E. A Review Article on Acrylic PMMA. *J. Mech. Civ. Eng.* **2016**, *13*, 1–4.
3. Ali, U.; Karim, K.J.B.A.; Buang, N.A. A Review of the Properties and Applications of Poly(Methyl Methacrylate) (PMMA). *Polym. Rev.* **2015**, *55*, 678–705. [[CrossRef](#)]
4. Puggal, S.; Dhall, N.; Singh, N.; Litt, M.S. A Review on Polymer Nanocomposites: Synthesis, Characterization and Mechanical Properties. *Ind. J. Sci. Technol.* **2016**, *9*, 1–4. [[CrossRef](#)]
5. Hussain, F.; Hojjati, M.; Okamoto, M.; Gorga, R.E. Review article: Polymer-matrix nanocomposites, processing, manufacturing and application: An overview. *J. Compos. Mater.* **2006**, *40*, 27–32. [[CrossRef](#)]

6. Chen, J.; Liu, B.; Gao, X.; Xu, D. A review of the interfacial characteristics of polymer nanocomposites containing carbon nanotubes. *RSC Adv.* **2018**, *8*, 28048–28085. [[CrossRef](#)]
7. Adeosun, S.O.; Lawal, G.I.; Balogun, S.A.; Akpan, E.I. Review of Green Polymer Nanocomposites. *J. Miner. Mater. Charact. Eng.* **2015**, *11*, 483–514. [[CrossRef](#)]
8. Zheng, J.; Zhu, R.; He, Z.; Cheng, G.; Wang, H.; Yao, K. Synthesis and Characterization of PMMA/SiO<sub>2</sub> Nanocomposites by In Situ Suspension Polymerization. *J. Appl. Polym. Sci.* **2010**, *115*, 1975–1981. [[CrossRef](#)]
9. Nasr, G.M.; Ahmed, R.M. AC conductivity and dielectric properties of PMMA/fullerene composites. *Mod. Phys. Lett. B* **2014**, *24*, 911–919. [[CrossRef](#)]
10. Motawie, A.M.; Madany, M.M.; El-dakrory, A.Z.; Osman, H.M. Physico-chemical characteristics of nano-organo bentonite prepared using different organo-modifiers. *Egypt. J. Pet.* **2014**, *23*, 331–338. [[CrossRef](#)]
11. Modak, S.K.; Mandal, A.; Chakrabarty, D. Studies on Synthesis and Characterization of Poly(methyl methacrylate)-Bentonite Clay Composite by Emulsion Polymerization and Simultaneous In Situ Clay Incorporation. *Polym. Compos.* **2013**, *34*, 32–40. [[CrossRef](#)]
12. Makvandi, P.; Nikfarjami, N.; Sanjani, N.S.; Qazvini, N.T. Effect of silver nanoparticle on the properties of poly (methyl methacrylate) nanocomposite network made by in situ photoiniferter-mediated photopolymerization. *Bull. Mater. Sci.* **2015**, *38*, 1625–1631. [[CrossRef](#)]
13. Logakis, E.; Pandis, C.; Pissis, P.; Pionteck, J.; Pötschke, P.; Logakis, E.; Pandis, C.; Pissis, P.; Pionteck, J.; Highly, P.P. Highly conducting poly (methyl methacrylate)/carbon nanotubes composites: Investigation on their thermal, dynamic-mechanical, electrical and dielectric properties. *Compos. Sci. Technol.* **2012**, *71*, 854–862. [[CrossRef](#)]
14. Safavi, F.; Malekie, S.; Ziaie, F. Electrical Conductivity Simulation of PMMA-CNT Nano-Composite in Different Frequencies. Presented at the Conference National Conference on Nanostructure and Graphene, Tehran, Iran, 27–28 May 2015.
15. Jordan, J.; Jacob, K.I.; Tannenbaum, R.; Sharaf, M.A.; Jasiuk, I. Experimental trends in polymer nanocomposites—A review. *Mater. Sci. Eng.* **2016**, *393*, 1–11. [[CrossRef](#)]
16. Lee, D.C.; Jang, L.W. Preparation and Characterization of PMMA-Clay Hybrid Composite by Emulsion Polymerization. *J. Appl. Polym. Sci.* **1996**, *61*, 1117–1122. [[CrossRef](#)]
17. Ray, S.S.; Okamoto, M. Polymer/layered silicate nanocomposites: A review from preparation to processing. *Prog. Polym. Sci.* **2003**, *28*, 1539–1641.
18. Amara, N.; Ayesha, K.; Ayesha, Y. A Review on Preparation, Properties and Applications of Polymeric Nanoparticle-Based Materials. *Polym. Technol. Eng.* **2015**, *54*, 325–341.
19. Morgan, A.B.; Gilman, J.W. An overview of flame retardance of polymeric materials: Application, technology, and future directions. *Fire Mater.* **2013**, *37*, 259–279. [[CrossRef](#)]
20. Camino, G.; Costa, L. Performance and mechanisms of fire retardants in polymers—A review. *Polym. Degrad. Stab.* **1988**, *20*, 271–294. [[CrossRef](#)]
21. Samujlo, B.; Rudawska, A. Influence of modification of low-density polyethylene with aluminium trihydroxide on its surface free energy. *Polimery* **2010**, *55*, 846–850. [[CrossRef](#)]
22. Sakiewicz, P.; Lutynski, M.; Soltys, J.; Pytlinski, A. Purification of halloysite by magnetic separation. *Physicochem. Probl. Miner. Process.* **2016**, *52*, 991–1001.
23. Chinellato, A.C.; Vidotti, S.E.; Hu, G.H.; Pessan, L.A. Compatibilizing effect of acrylic acid modified polypropylene on the morphology and permeability properties of polypropylene/organoclay nanocomposites. *Compos. Sci. Technol.* **2010**, *70*, 458–465. [[CrossRef](#)]
24. Alexandre, M.; Dubois, P. Polymer-layered silicate nanocomposites: Preparation, properties and uses of a class of materials. *Mater. Sci. Eng.* **2000**, *28*, 1–63. [[CrossRef](#)]
25. Rong, M.Z.; Zhang, M.Q.; Pan, S.L.; Lehmann, B.; Friedrich, K. Analysis of the interfacial interactions in polypropylene/silica nanocomposites. *Polym. Int.* **2004**, *53*, 176–183. [[CrossRef](#)]
26. Lim, J.S.; Noda, I.; Im, S.S. Effect of hydrogen bonding on the crystallization behavior of poly(3-hydroxybutyrate-co-3-hydroxyhexanoate)/silica hybrid composites. *Polymer* **2007**, *48*, 2745–2754. [[CrossRef](#)]
27. Prashantha, K.; Lacrampe, M.F.; Krawczak, P. Processing and characterization of halloysite nanotubes filled polypropylene nanocomposites based on a masterbatch route: Effect of halloysites treatment on structural and mechanical properties. *Exp. Polym. Lett.* **2011**, *5*, 295–307. [[CrossRef](#)]

28. Luo, B.H.; Wen, W.; Xie, W.J.; Zhang, J.X.; Liu, M.X.; Zhou, C.R. Modified Halloysite Nanotube/Biodegradable Polyester Composite Material and Preparation Method Thereof. CN Patent 102952385A, 6 March 2013.
29. Luo, B.H.; Wen, W.; Xie, W.J.; Zhang, J.X.; Liu, M.X. Modified Halloysite Nanotube/Biodegradable Polyester Composite Material and Preparation Method Thereof. CN Patent 102952385B, 4 June 2014.
30. Mills, D.; Lvov, Y.M. Ceramic Nanotube Composites with Sustained Drug Release Capability for Implants, Bone Repair and Regeneration. U.S. Patent 9192912B1, 24 November 2015.
31. Kausch, C.; Verrocchi, A.; Pomeroy, J.E., III; Peterson, K.M.; Payne, P.F. Flame Resistant Polyolefin Compositions Containing Organically Modified Clay. U.S. Patent 6414070B1, 2 July 2006.
32. Weil, E.D.; Levchik, S.V. Commercial flame retardancy of unsaturated polyester and vinyl resins: Review. *J. Fire Sci.* **2004**, *22*, 293–303. [[CrossRef](#)]
33. Chung, J.Y.; Paul, W.G. Flame Retardant Hydrotalcite Containing Polycarbonate Compositions. PCT Patent WO2003046067A1, 5 June 2003.
34. Sheist, I. *Handbook of Adhesives*, 3rd ed.; Chapman & Hall, International Thomson Publishing: New York, NY, USA, 1990.
35. Kango, S.; Kalia, S.; Celli, A.; Njuguna, J.; Habibi, Y.; Kumar, R. Surface modification of inorganic nanoparticles for development of organic–inorganic nanocomposites—A review. *Prog. Polym. Sci.* **2013**, *38*, 1232–1261. [[CrossRef](#)]
36. Xie, Y.; Hill, C.A.S.; Xiao, Z.; Militz, H.; Mai, C. Silane coupling agents used for natural fiber/polymer composites: A review. *Compos. Part A Appl. Sci. Manuf.* **2010**, *41*, 806–819. [[CrossRef](#)]
37. Carli, L.N.; Daitz, T.S.; Soares, G.V.; Crespo, J.S.; Mauler, R.S. The effects of silane coupling agents on the properties of PHBV/halloysite nanocomposites. *Appl. Clay Sci.* **2014**, *87*, 311–319. [[CrossRef](#)]
38. Khunova, V.; Kristóf, J.; Kelnar, I.; Dybal, J. The effect of halloysite modification combined with in situ matrix modifications on the structure and properties of polypropylene/halloysite nanocomposites. *Exp. Polym. Lett.* **2013**, *7*, 471–479. [[CrossRef](#)]
39. Dong, Y.; Marshall, J.; Haroosh, H.J.; Mohammadzadehmoghadam, S.; Liu, D.; Qi, X.; Lau, K.T. Polylactic acid (PLA)/halloysite nanotube (HNT) composite mats: Influence of HNT content and modification. *Compos. Part A Appl. Sci. Manuf.* **2015**, *76*, 28–36. [[CrossRef](#)]
40. Barrientos-Ramírez, S.; De Oca-Ramírez, G.M.; Ramos-Fernández, E.V.; Sepúlveda-Escribano, A.; Pastor-Blas, M.M.; González-Montiel, A. Surface modification of natural halloysite clay nanotubes with aminosilanes. Application as catalyst supports in the atom transfer radical polymerization of methyl methacrylate. *Appl. Catal. A Gen.* **2011**, *406*, 22–33. [[CrossRef](#)]
41. Joussein, E.; Petit, S.; Delvaux, B. Behavior of halloysite clay under formamide treatment. *Appl. Clay Sci.* **2007**, *35*, 17–24. [[CrossRef](#)]
42. Joussein, E.; Petit, S.; Churchman, J.; Theng, B.; Righi, D.; Delvaux, B. Halloysite clay minerals—A review. *Clay Miner.* **2005**, *40*, 383–426. [[CrossRef](#)]
43. Adjuvants Help Vaccines Work Better. Available online: <https://www.cdc.gov/vaccinesafety/concerns/adjuvants.html> (accessed on 22 February 2019).
44. Tyliczszak, B.; Drabczyk, A.; Drabczyk, A.; Kudłacik-kramarczyk, S. Acrylates in Dental Applications. In *Acrylic Polymers in Healthcare*; Reddy, B., Ed.; IntechOpen: Rijeka, Croatia, 2017; pp. 25–42.
45. Ma, S.; Song, G.; Zhong, L.; Tang, G. Study on Bulk Polymerization of Methyl Methacrylate initiated by low intensity ultrasonic irradiation. *J. Appl. Polym. Sci.* **2010**, *116*, 3127–3133. [[CrossRef](#)]
46. Schouten, A. Bulk polymerization of Methyl Methacrylate in the presence of Poly(Methyl Methacrylate). II. Effect of oxygen. *J. Polym. Sci.* **1974**, *12*, 2145–2147. [[CrossRef](#)]
47. Tong, J.; Ma, Y.; Jiang, M. Effects of the wollastonite fiber modification on the sliding wear behavior of the UHMWPE composites. *Wear* **2003**, *255*, 734–741. [[CrossRef](#)]
48. Ha, S.R.; Ryu, S.H.; Park, S.J.; Rhee, K.Y. Effect of clay surface modification and concentration on the tensile performance of clay/epoxy nanocomposites. *Mater. Sci. Eng. A* **2007**, *448*, 264–268. [[CrossRef](#)]
49. Liu, G.; Zhou, B.; Li, Y.; Qi, T.; Li, X. Surface properties of superfine alumina trihydrate after surface modification with stearic acid. *Int. J. Miner. Metall. Mater.* **2015**, *22*, 537–543. [[CrossRef](#)]
50. Izabella, L.; Al-Zahari, M.; Ewa, W.; Osawaru, O. The method of obtaining the modifier for polymers and polymer nanocomposites. PL Patent 213268, 16 September 2011.

51. Kavooosi, G.; Mahdi Dadfar, S.M.; ALi, D.S.M.; Niakousari, M. Investigation of gelatin/multi-walled carbon nanotube nanocomposite films as packaging materials. *Food Sci. Nutr.* **2014**, *2*, 65–73. [[CrossRef](#)] [[PubMed](#)]
52. Richards, S.R.; Turner, R.J. A comparative study of techniques for the examination of biofilms by scanning electron microscopy. *Water Res.* **1984**, *18*, 676–773. [[CrossRef](#)]
53. Maczynska, B.; Neumann, K.; Junka, A.; Smutnicka, D.; Secewicz, A.; Bartoszewicz, M.; Wojkowska-Mach, J.; Sekowska, A.; Gospodarek, E.; Burdynowski, K. Analysis of properties related to selection and survival in hospital environment of Klebsiella strains isolated from nosocomial outbreaks. *Forum Zakaz.* **2013**, *4*, 77–97.
54. Barrientos-Ramírez, S.; Ramos-Fernández, E.V.; Silvestre-Albero, J.; Sepúlveda-Escribano, A.; Pastor-Blas, M.M.; González-Montiel, A. Use of nanotubes of natural halloysite as catalyst support in the atom transfer radical polymerization of methyl methacrylate. *Microporous Microporous Mater.* **2009**, *120*, 132–140. [[CrossRef](#)]
55. Yuan, P.; Southon, P.D.; Liu, Z.; Green, M.E.R.; Hook, J.M.; Antill, S.J.; Kepert, C.J. Functionalization of Halloysite Clay Nanotubes by Grafting with  $\gamma$ -Aminopropyltriethoxysilane. *J. Phys. Chem. C* **2008**, *112*, 15742–15751. [[CrossRef](#)]
56. Li, Y.; Li, R.; Fu, X.; Wang, Y.; Zhong, W. A bio-surfactant for defect control: Multifunctional gelatin coated MWCNTs for conductive epoxy nanocomposites A bio-surfactant for defect control: Multifunctional gelatin coated MWCNTs for conductive epoxy nanocomposites. *Compos. Sci. Technol.* **2018**, *159*, 216–224. [[CrossRef](#)]
57. George, G.; Selvakumar, M.; Mahendran, A.; Anandhan, S. Structure-property relationship of halloysite nanotubes/ethylene-vinyl acetate-carbon monoxide terpolymer nanocomposites. *J. Thermoplast. Compos. Mater.* **2017**, *30*, 121–140. [[CrossRef](#)]
58. Dhibar, S.; Das, C.K. Silver Nanoparticles Decorated Polyaniline/Multiwalled Carbon Nanotubes Nanocomposite for High-Performance Supercapacitor Electrode. *Ind. Eng. Chem. Res.* **2014**, *53*, 3495–3508. [[CrossRef](#)]
59. Mombeshora, E.T.; Simoyi, R.; Nyamori, V.O.; Ndungu, P.G. Multiwalled carbon nanotube-titania nanocomposites: Understanding nano-structural parameters and functionality in dye-sensitized solar cells. *S. Afr. J. Chem.* **2015**, *68*, 153–164. [[CrossRef](#)]
60. Pal, K.; Banthia, A.K.; Majumdar, D.K. Preparation and characterization of polyvinyl alcohol-gelatin hydrogel membranes for biomedical applications. *AAPS Pharm. Sci. Technol.* **2007**, *8*, E1–E5. [[CrossRef](#)]
61. Massoumi, B.; Hosseinzadeh, M.; Jaymand, M. Electrically conductive nanocomposite adhesives based on epoxy or chloroprene containing polyaniline, and carbon nanotubes. *J. Mater. Sci. Mater. Electron.* **2015**, *26*, 6057–6067. [[CrossRef](#)]
62. König, A.; Malek, A.; Fehrenbacher, U.; Brunklaus, G.; Wilhelm, M.; Hirth, T. Silane-functionalized Flame-retardant Aluminum Trihydroxide in Flexible Polyurethane Foam. *J. Cell. Plast.* **2010**, *46*, 395–413. [[CrossRef](#)]
63. Soares, V.L.P.; Nascimento, R.S.V.; Menezes, V.J.; Batista, L. TG characterization of organically modified montmorillonite. *J. Therm. Anal. Calorim.* **2004**, *75*, 671–676. [[CrossRef](#)]
64. Plueddemann, E.P. *Silane Coupling Agents*, 2nd ed.; Springer Science +Business Media: Berlin, Germany, 1991.
65. Zhu, L.; Pu, S.; Lu, F.; Liu, K.; Zhu, T.; Li, J.; Li, J. Preparation of dispersed aluminum hydroxide nanoparticles via non-aqueous route and surface modification. *Mater. Chem. Phys.* **2012**, *135*, 979–984. [[CrossRef](#)]
66. Ibrahim, D.M.; Abu-Ayana, Y.M. Preparation and characterization of ultrafine alumina via sol-gel polymeric route. *Mater. Chem. Phys.* **2008**, *111*, 326–330. [[CrossRef](#)]
67. Liu, M.; Jia, Z.; Jia, D.; Zhou, C. Recent advance in research on halloysite nanotubes-polymer nanocomposite. *Prog. Polym. Sci.* **2014**, *39*, 1498–1525. [[CrossRef](#)]
68. Valdez-Salas, B.; Beltrán-Partida, E.; Nedeve, N. Controlled antifungal behavior on Ti6Al4V nanostructured by chemical nanopatterning. *Mater. Sci. Eng. C Mater. Biol. Appl.* **2019**, *96*, 677–683. [[CrossRef](#)] [[PubMed](#)]
69. Vilarrasa, J.; Delgado, L.M.; Galofré, M.; Álvarez, G.; Violant, D.; Manero, J.M.; Blanc, V.; Gil, F.J.; Nart, J. In vitro evaluation of a multispecies oral biofilm over antibacterial coated titanium surfaces. *J. Mater. Sci. Mater. Med.* **2018**, *29*, 164. [[CrossRef](#)]
70. Li, Z.; Sun, J.; Lan, J.; Qi, Q. Effect of a denture base acrylic resin containing silver nanoparticles on Candida albicans adhesion and biofilm formation. *Gerontology* **2016**, *33*, 209–216.
71. Shu, Z.; Zhang, Y.; Yang, Q.; Yang, H. Halloysite Nanotubes Supported Ag and ZnO Nanoparticles with Synergistically Enhanced Antibacterial Activity. *Nanoscale Res. Lett.* **2017**, *12*, 135. [[CrossRef](#)] [[PubMed](#)]

72. Yu, L.; Zhang, Y.; Zhang, B.; Liu, J. Enhanced antibacterial activity of silver nanoparticles/halloysite nanotubes/graphene nanocomposites with Sandwich-like structure. *Sci. Rep.* **2014**, *4*, 4551. [[CrossRef](#)] [[PubMed](#)]
73. Cervini-Silva, J.; Nieto-Camacho, A.; Palacios, E.; Montoya, J.A.; Gomez-Vidales, V.; Ramirez-Tapan, M.T. Anti-inflammatory and anti-bacterial activity, and cytotoxicity of halloysite surfaces. *Colloids Surf. B Biointerfaces* **2013**, *111*, 651–655. [[CrossRef](#)] [[PubMed](#)]



© 2019 by the authors. Licensee MDPI, Basel, Switzerland. This article is an open access article distributed under the terms and conditions of the Creative Commons Attribution (CC BY) license (<http://creativecommons.org/licenses/by/4.0/>).